

Hydrogen Donors in ZnO

M.D. McCluskey, S.J. Jokela, and W.M. Hlaing Oo
Department of Physics, Washington State University,
Pullman, WA 99164-2814, U.S.A.

ABSTRACT

Zinc oxide (ZnO) has shown great promise as a wide-bandgap semiconductor with a range of optical, electronic, and mechanical applications. The presence of compensating donors, however, is a major roadblock to achieving *p*-type conductivity. Recent first-principles calculations and experimental studies have shown that hydrogen acts as a shallow donor in ZnO, in contrast to hydrogen's usual role as a passivating impurity. Given the omnipresence of hydrogen during growth and processing, it is important to determine the structure and stability of hydrogen donors in ZnO.

To address these issues, we performed vibrational spectroscopy on bulk, single-crystal ZnO samples annealed in hydrogen (H₂) or deuterium (D₂) gas. Using infrared (IR) spectroscopy, we observed O-H and O-D stretch modes at 3326.3 cm⁻¹ and 2470.3 cm⁻¹ respectively, at a sample temperature of 10 K. These frequencies indicate that hydrogen forms a bond with a host oxygen atom, consistent with either an antibonding or bond-centered model. In the antibonding configuration, hydrogen attaches to a host oxygen and points away from the Zn-O bond. In the bond-centered configuration, hydrogen sits between the Zn and O. To discriminate between these two models, we measured the shift of the stretch-mode frequency as a function of hydrostatic pressure. By comparing with first-principles calculations, we conclude that the antibonding model is the correct one.

Surprisingly, we found that the O-H complex is unstable at room temperature. After a few weeks, the peak intensity decreases substantially. It is possible that the hydrogen forms H₂ molecules, which have essentially no IR signature. Electrical measurements show a corresponding decrease in electron concentration, which is consistent with the formation of neutral H₂ molecules. The correlation between the electrical and spectroscopic measurements, however, is not perfect. We therefore speculate that there may be a second "hidden" hydrogen donor. One candidate for such a donor is a hydrogen-decorated oxygen vacancy.

Table I. Band gaps of several important wide-band-gap semiconductors. Energies are given in eV (nm). The cubic structure for GaN and AlN is zincblende. The hexagonal structure for GaN, AlN, and ZnO is wurtzite. 4H, 6H, and 2H denote the hexagonal polytypes of SiC.

| GaN | SiC | ZnO | Diamond |
|----------------------|-----------------|---------------------|-----------------|
| Cubic 3.27 (379) | Cubic 2.2 (537) | Hexagonal 3.3 (376) | Cubic 5.4 (230) |
| Hexagonal 3.47 (357) | 4H 3.27 (379) | | |
| | 6H 2.9 (428) | | |
| | 2H 3.3 (376) | | |

INTRODUCTION

Zinc Oxide – a wide-band-gap semiconductor

The past decade has seen dramatic advances in the development of wide-band-gap semiconductors (Table I) for electronic and optoelectronic applications [1,2]. Gallium nitride (GaN) has emerged as a leading material for light-emitting diodes (LEDs) and laser diodes in the blue-to-ultraviolet (UV) region of the spectrum [1,3]. GaN, silicon carbide (SiC), and diamond have been proposed as materials in electronic devices for high-power, high-temperature, and high-frequency applications [4,5,6]. The technological advances have been supported by fundamental research into the structural, optical, electronic, and defect properties of these materials. Despite impressive successes, however, significant materials problems still exist. Due to the high volatility of nitrogen, GaN cannot be grown in truly bulk quantities [7], nor is it amenable to inexpensive thin-film growth techniques such as sputter deposition [8]. Bipolar SiC devices suffer from degradation during operation due to the propagation of extended defects [9]. Diamond, a promising wide-band-gap semiconductor, is resistant to *n*-type doping [10].

Due to these and other problems, the investigation of alternative materials systems is an important research activity. Zinc oxide (ZnO) is a semiconductor that has attracted resurgent interest as an electronic material for a range of applications [11]. A wide-band-gap semiconductor, ZnO emits light in the blue-to-UV region of the spectrum. The efficiency of the emission is higher than more conventional materials such as GaN [12], making ZnO a strong candidate for energy-efficient white lighting. Another major advantage of ZnO is the fact that, in contrast to GaN, large single crystals can be grown [13]. ZnO has been used as a transparent conductor [14] in solar cells [15], and is a preferred material in transparent transistors, “invisible” devices which could be very useful in products such as liquid-crystal displays [16].

In addition to optoelectronic and electronic devices, ZnO has emerged as a potentially important material for spintronic applications [17,18,19]. In quantum computing devices, the spin states of impurities or charge carriers would be used to construct “qubits,” theoretically enabling the manipulation of huge amounts of data [20]. For non-volatile memory storage applications, ferromagnetism is used to store data for extended periods of time [21]. Semiconductors such as ZnO offer the possibility of devices that combine optical and magnetic effects, such as spin LEDs [22,23,24,25], spin-polarized solar cells [26], and magneto-optical switches [27]. The development of room-temperature ferromagnetic materials will be essential for the practical realization of these technologies. Theoretical work has predicted ferromagnetism above room temperature for Mn-doped ZnO, given a high hole concentration [28], an important requirement for spintronic devices. Spurred by that prediction, research into ZnO crystals for spintronic applications is an active area of experimental research [29].

The problem: p-type doping

In spite of its numerous advantages and potential applications, ZnO suffers from one major drawback: as grown, it contains a relatively high level of donor defects. These defects and impurities compensate acceptors or donate free electrons to the conduction band, making ZnO *n*-type. Reliable *p*-type doping, where current is carried by free holes, has not been achieved. The lack of *p*-type conductivity has prevented ZnO from competing with other wide-band-gap

semiconductors. In order to overcome that obstacle, the role of donor impurities in ZnO must be understood. In addition, novel schemes for introducing acceptor dopants must be investigated if ZnO-based devices are to become technologically feasible.

Hydrogen: a shallow donor in ZnO

Several decades after the experimental studies of Mollwo [30] and Thomas and Lander [31], first-principles calculations by Van de Walle [32] demonstrated that hydrogen could be a shallow donor in ZnO, raising the possibility that hydrogen donors may be introduced into the bulk during growth or processing. Spurred by the theoretical predictions, experiments on muonium implanted into ZnO [33] and electron-nuclear resonance measurements on *n*-type ZnO [34] supported the claim that hydrogen is indeed a shallow donor.

In order to determine the microscopic structure of hydrogen donors, in previous work, we used infrared (IR) spectroscopy to measure the local vibrational modes (LVMs) arising from these complexes [35]. Although it was established conclusively that hydrogen forms O-H complexes, the microscopic structure of these complexes was not known. Two possible models for the O-H complex are shown in Figure 1: the antibonding (AB_{\perp}) and bond-centered (BC_{\perp}) configurations. In both of the models shown in the Figure, the O-H bond is oriented at a nearly tetrahedral angle with respect to the *c* axis. However, theoretical studies also proposed AB_{\parallel} and BC_{\parallel} configurations, where the O-H bond is parallel to the *c* axis. Since the LVM frequencies for all of these models are similar, further experiments were required to identify the correct one.

In this article, recent results from our group are reviewed, based in part on Refs. 35, 36, and 37. Recent work by Nickel *et al.* [38], Lavrov *et al.* [39,40], and Halliburton *et al.* [41] have reported hydrogen-related LVMs that are different from what is reported here.

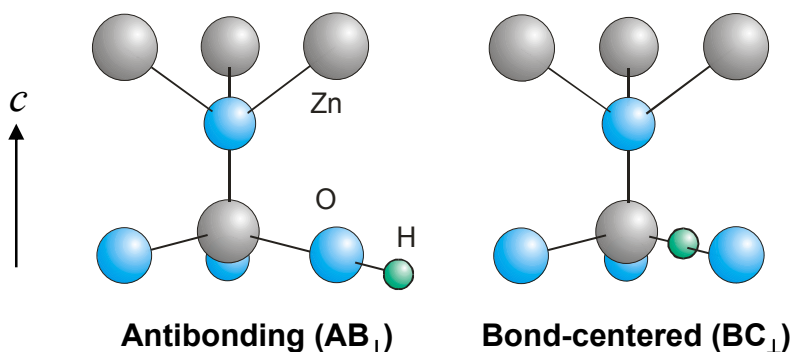


Figure 1. Two possible models for hydrogen donors in ZnO. Theoretically, the O-H complexes may also be aligned along the *c* axis.

EXPERIMENTAL DETAILS

Single crystal, *c*-cut samples of ZnO with a thickness of 0.5 mm were purchased from Cermet, Inc. The as-received samples had a free-electron concentration of $n \sim 2 \times 10^{17} \text{ cm}^{-3}$. Some samples were sealed inside a quartz ampoule, evacuated and backfilled with 2/3 atm of hydrogen gas. The ampoule also contained ZnO powder, in order to minimize the reduction of

ZnO by hydrogen at high temperatures. The ampoule was placed in a furnace and annealed in the temperature range of 700-800°C for several hours. The ampoule was then quenched to room temperature by immersion in water, and the sample was retrieved by breaking the ampoule. Following the hydrogen diffusion process, the free-electron concentration increased to $4\text{-}5 \times 10^{17} \text{ cm}^{-3}$. The increase in free electrons is consistent with the claim that hydrogen in ZnO is a shallow donor.

Room-temperature Hall-effect measurements (MMR Technologies, Inc.) were performed in the van der Pauw geometry, using a 1 Tesla electromagnet. IR spectroscopy was performed using a vacuum Fourier transform IR (FTIR) spectrometer (Bomem DA8) and an InSb detector. The O-H LVM was measured at room temperature and liquid-helium temperatures ($\sim 10 \text{ K}$). For the low temperature measurements, a liquid-helium continuous-flow cryostat with wedged ZnSe windows was used (Janis STVP).

DISCUSSION

Local vibrational modes

Using infrared IR spectroscopy, we have observed O-H and O-D stretch modes at 3326.3 cm^{-1} (Figure 2) and 2470.3 cm^{-1} (not shown) respectively, at a sample temperature of 8 K. The isotopic frequency ratio is in agreement with what one would expect from an O-H complex. As the temperature is increased, the LVM width *and* frequency increase.

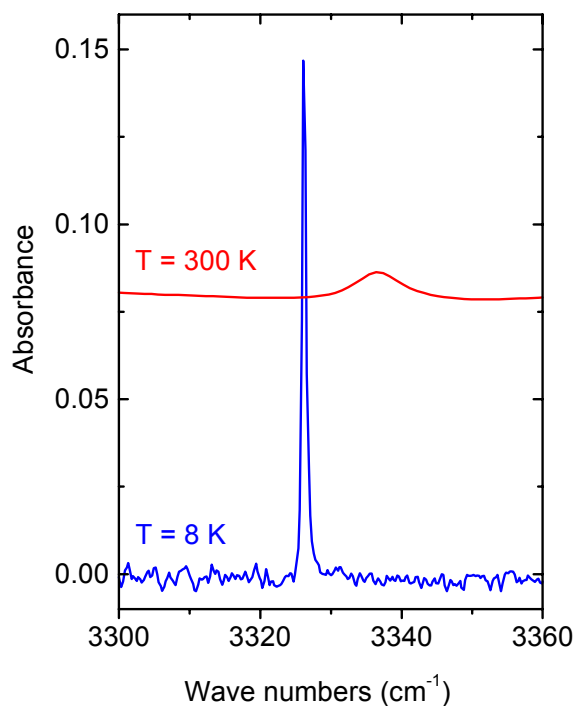


Figure 2. IR absorption spectra of O-H complexes in ZnO, at a temperature of 8 and 300 K.

Polarized IR spectroscopy

The IR measurements described in the previous section were performed in a normal incidence geometry on *c*-cut ZnO samples. Since the polarization of the light is perpendicular to the *c* axis, it follows that the O-H complexes that we observed are *not* aligned along the *c* axis. This observation contradicts some theoretical reports, which claim that the lowest energy orientation of the hydrogen is in the BC_{//} configuration [32]. The calculated energy differences are small, however, on the order of 0.1 eV.

To check this result, we performed polarized IR spectroscopy on an *a*-cut sample. For light that was polarized along the *c* axis, the O-H absorption is reduced as compared to light perpendicular to the *c* axis. As discussed in Ref. 37, our results are consistent with O-H dipoles that are aligned at an angle of $\sim 112^\circ$ to the *c* axis. Additional experiments, to be published later, have confirmed that the O-H dipoles are aligned at a tetrahedral angle with respect to the *c* axis. In other words, our results are consistent with the AB_⊥ or BC_⊥ models.

High-pressure IR spectroscopy

Regarding the structure of the O-H complexes, one question remains: is the configuration bond-centered or anti-bonding? Since both structures have identical symmetry, it is not obvious how to distinguish between them. One possible method involves measuring the O-H stretch-mode frequency as a function of hydrostatic pressure. By comparing the results with predictions of *ab initio* calculations, it should be possible to determine the structure with reasonable certainty.

Following this strategy, high-pressure measurements were performed at liquid-helium temperatures, using a diamond-anvil cell. As shown in Figure 3, there is only a very slight shift with pressure, approximately $-1 \text{ cm}^{-1}/\text{GPa}$. Qualitatively, this small shift would seem to favor the antibonding orientation, in which the hydrogen is not crowded by neighboring atoms. However, it will be necessary to compare our results with first-principles calculations.

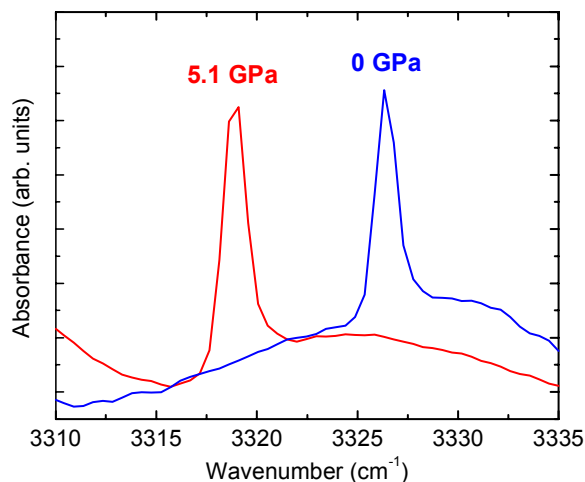


Figure 3. IR spectra of ZnO:H under pressure.

Instability of O-H complexes

At room temperature, the O-H complexes are unstable: after a few weeks or months, the intensity of the IR peak decreases significantly. In order to explore this decay process in detail, two identical hydrogenated samples were prepared. For one sample, the electron concentration was measured as a function of time, with the room-temperature Hall-effect apparatus. For the other sample, room-temperature IR spectroscopy was performed to measure the intensity of the O-H LVM peak. The results of these measurements are plotted in Figure 4, where the circles and squares refer to the Hall-effect and IR data, respectively.

It is clear that the decay of the O-H peak and the decay of the free-electron concentration are well correlated, providing evidence that the O-H complexes are shallow donors. The data were fit using a biexponential decay model,

$$N = \frac{1}{1/N_0 + At} \quad (1)$$

where N is the number of O-H complexes, N_0 and A are adjustable parameters, and t is time. This model is consistent with the idea that hydrogen donors may form H_2 molecules [48]. Since H_2 molecules are essentially IR inactive, and electrically neutral, the formation of H_2 molecules results in a decrease in the O-H IR mode *and* free-electron concentration.

Although the correlation between the O-H LVM and the free-electron concentration is good, it is not perfect. For long times, the O-H LVM approaches zero intensity. The free-electron concentration, however, approaches a constant value that is slightly higher than the as-received free-electron concentration. Therefore, it appears that there are some “invisible” hydrogen donors which are stable at room temperature. This result is consistent with the work of Shi *et al.* [48], who showed that a fraction of the hydrogen donors persist after annealing at temperatures below 500°C.

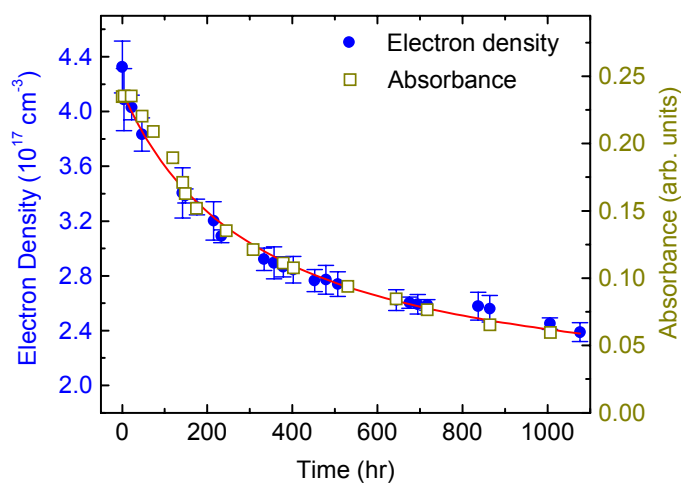


Figure 4. Decay of free-electron density (circles) and OH-peak absorbance (squares) as a function of time, at room temperature.

Hydrogen in ZnO nanoparticles

Our research on impurities in ZnO has been extended from bulk crystals to nanoparticles. The use of nanoscale semiconductors provides several advantages over bulk materials. First, the electronic and optical properties can be tuned by varying the size of the nanoparticle [49,50]. Second, nanoparticles can be embedded in a matrix, which can be made into fibers or other technologically useful forms [51]. Finally, by reducing the spatial dimensions to the nanoscale, high storage densities may be achieved by addressing the spin states of single quantum dots [52]. From a fundamental point of view, the study of nanoparticles provides insight into the mesoscopic regime between single molecules and bulk crystals.

As the spatial dimension of the ZnO semiconductor crystals approach the nanoscale, one can expect that the increase in surface-to-volume ratio will result in different impurity behavior. To explore this difference, we studied the effect of hydrogen impurities on the IR and electrical properties of ZnO nanoparticles. The ZnO nanoparticles were synthesized by wet-chemical techniques, as described in Ref. 53. The particles were roughly spherical, with an average diameter of ~ 20 nm (Figure 5). The nano-powder was pressed into pellets with thicknesses of ~ 0.25 mm. Some samples were then annealed in hydrogen gas at a temperature of 350°C .

As shown in Figure 6, the conductivity of the ZnO pellets increased by several orders of magnitude after hydrogenation. This dramatic increase in conductivity was accompanied by a large increase in free-carrier absorption (Figure 7). Both of these observations are consistent with a model in which hydrogen donors diffuse into the ZnO nanoparticles. With bulk ZnO, a similar annealing temperature does not affect the conductivity significantly. ZnO nanoparticles, on the other hand, have an extremely high surface-to-volume ratio which may allow hydrogen to rapidly permeate at moderate annealing temperatures.

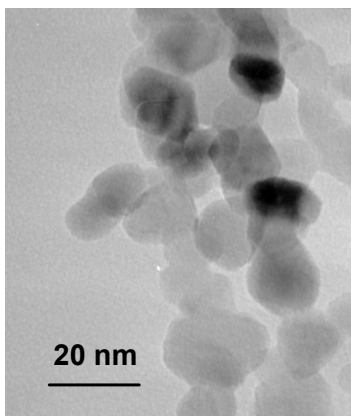


Figure 5. Transmission electron microscope (TEM) image of ZnO nanoparticles.

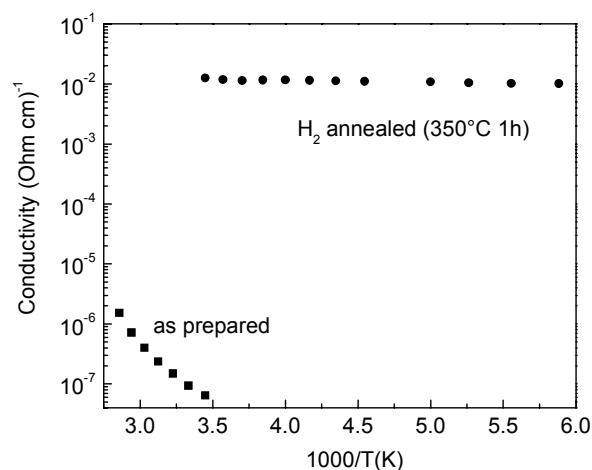


Figure 6. Conductivity of pellets of ZnO nanoparticles, as prepared and annealed in H₂.

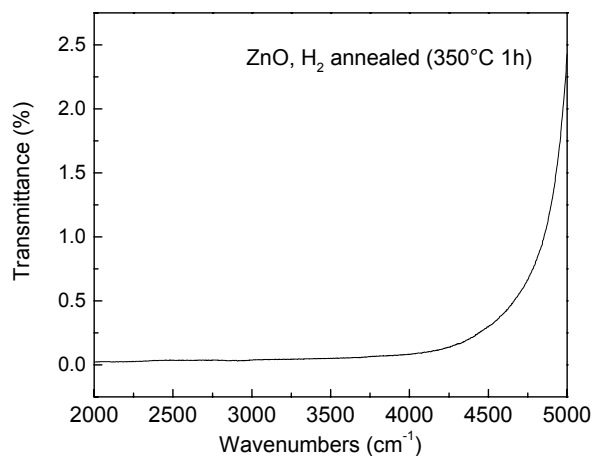


Figure 7. Free-carrier absorption of ZnO annealed in H₂.

CONCLUSIONS

Hydrogen donors have been characterized in bulk and nanoscale ZnO. In bulk samples annealed in hydrogen, O-H donor complexes are formed. By performing polarized IR and high-pressure IR spectroscopy, we conclude that the O-H donors are in the AB_⊥ configuration. These donors are unstable – at room temperature, they decay significantly over a few weeks. The IR and electrical data are consistent with the idea that most of the O-H donors form neutral H₂ molecules in the ZnO crystal. However, a fraction of the O-H donors may transform into donor that is “invisible” to our IR measurements. One candidate for such an anonymous donor is a hydrogen-decorated oxygen vacancy, which would have a low-frequency mode, outside the spectral range of our measurements [54].

In ZnO nanoparticles, at moderate annealing temperatures (350°C), hydrogen permeates the nanoparticles, resulting in a dramatic increase in electrical conductivity, free-carrier absorption, and infrared reflectivity. These results could be relevant to hydrogen sensing and storage applications.

ACKNOWLEDGMENTS

The authors would like to thank M. Stavola and C.G. Van de Walle for helpful discussions. This work was supported in part by the National Science Foundation under Grant No. DMR-0203832. Acknowledgment is made to the Donors of the American Chemical Society Petroleum Research Fund for partial support of this research.

REFERENCES

1. N.M. Johnson, A.V. Nurmikko, and S.P. DenBaars, *Physics Today* **53** (10), 31-6 (2000).
2. A.R. Powell and L.B. Rowland, *Proc. IEEE* **90**, 942-55 (2002).
3. S. Nakamura, *Physica Status Solidi A* **176**, 15-22 (1999).
4. S.J. Pearton *et al.*, *Mat. Sci. Engin. B* **82**, 227-31 (2001).
5. Y. Sugawara, *Mater. Sci. Forum* **457-60**, 963-8 (2004).
6. W. Ebert and E. Kohn, *Semicond. Sci. Tech.* **18**, S59-S66 (2003).
7. R. Czernetzki *et al.*, *Physica Status Solidi A* **200**, 9-12 (2003).
8. J.H. Kim, N. Shepherd, M. Davidson, and P.H. Holloway, *Appl. Phys. Lett.* **83**, 641-3 (2003).
If a “bulk” GaN target is used, then sputter deposition of GaN is possible. However, bulk GaN is itself quite expensive, in contrast to ZnO.
9. H. Lendenmann, J.P. Bergman, F. Dahlquist, and C. Hallin, *Mater. Sci. Forum* **433**, 901-6 (2002).
10. S. Koizumi, “N-type diamond growth,” *Semiconductors and Semimetals* **76**, 239-59 (2003).
11. S.J. Pearton, D.P. Norton, K. Ip, Y.W. Heo, and T. Steiner, *Journ. Vacuum Sci. Tech B* **22**, 932-48 (2004).
12. D.C. Look, *Mater. Sci. Engin. B* **80**, 383-7 (2001).
13. J.M. Ntep, S.S. Hassani, A. Lusson, A. Tromson-Carli, D. Ballutaud, G. Didier, and R. Triboulet, *Journ. Crystal Growth* **207**, 30-4 (1999).
14. T. Minami, *MRS Bulletin* **25** (8), 38-44 (2000).
15. A. Nuruddin and J.R. Abelson, *Thin Solid Films* **394**, 49-63 (2001).
16. J.F. Wager, *Science* **300**, 1245-6 (2003).
17. G.A. Prinz, *Science* **282**, 1660-3 (1998).
18. T. Dietl and H. Ohno, *MRS Bulletin* **28** (10), 714-9 (2003).
19. S.K. Kamilla and S. Basu, *Bull. Mater. Sci.* **25**, 541-3 (2002).
20. A. Steane, *Reports on Progress in Physics* **61**, 117-73 (1998).
21. S. Parkin, X. Jiang, C. Kaiser, A. Panchula, K. Roche, and M. Samant, *Proceedings of the IEEE* **91**, 661-80 (2003).
22. B.T. Jonker, Y.D. Park, B.R. Bennett, H.D. Cheong, G. Kiosoglou, and A. Petrou, *Phys. Rev. B* **62**, 8180-3 (2000).
23. Y. Ohno, D.K. Young, B. Beschoten, F. Matsukura, H. Ohno, and D.D. Awschalom, *Nature* **402**, 790-2 (1999).
24. J.M. Kikkawa and D.D. Awschalom, *Nature* **397**, 139-41 (1999).
25. R. Fiederling, M. Keim, G. Reuscher, W. Ossau, G. Schmidt, A. Waag, and L.W. Molenkamp, *Nature* **402**, 787-90 (1999).
26. I. Zutic, J. Fabian, and S. Das Sarma, *Phys. Rev. B* **64**, 121201 (2001).
27. Y.S. Didosyan, H. Hauser, G.A. Reider, and W. Toriser, *J. Appl. Phys.* **95**, 7339-41 (2004).
28. T. Dietl, H. Ohno, F. Matsukura, J. Cibert, and D. Ferrand, *Science* **287**, 1019-22 (2000).
29. P. Sharma, A. Gupta, K.V. Rao, F.J. Owens, R. Sharma, R. Ahuja, J.M. Osorio Guillen, Börje Johansson, and G.A. Gehring, *Nature Materials* **2**, 673-7 (2003).
30. E. Mollwo, *Z. Phys.* **138**, 478 (1954).
31. D.G. Thomas and J.J. Lander, *J. Chem. Phys.* **25**, 1136 (1956).
32. C.G. Van de Walle, *Phys. Rev. Lett.* **85**, 1012 (2000).

33. S.F.J. Cox, E.A. Davis, S.P. Cottrell, P.J.C. King, J.S. Lord, J.M. Gil, H.V. Alberto, R.C. Vilão, J. Piroto Duarte, N. Ayres de Campos, A. Weidinger, R.L. Lichti, and S.J.C. Irvine, *Phys. Rev. Lett.* **86**, 2601 (2001).
34. D.M. Hoffman, A. Hofstaetter, F. Leiter, H. Zhou, F. Henecker, B.K. Meyer, S.B. Orlinskii, J. Schmidt, and P.G. Baranov, *Phys. Rev. Lett.* **88**, 045504 (2002).
35. M.D. McCluskey, S.J. Jokela, K.K. Zhuravlev, P.J. Simpson, and K.G. Lynn, *Appl. Phys. Lett.* **81**, 3807 (2002).
36. M.D. McCluskey and S.J. Jokela, in MRS Proc. Vol. **813**, edited by N.H. Nickel, M.D. McCluskey, and S.B. Zhang (Materials Research Society, PA, 2004).
37. S.J. Jokela, M.D. McCluskey, and K.G. Lynn, *Physica B* **340-342**, 221 (2003).
38. N.H. Nickel and K. Fleischer, *Phys. Rev. Lett.* **90**, 197402 (2003).
39. E.V. Lavrov, J. Weber, F. Börrnert, C.G. Van de Walle, R. Helbig, *Phys. Rev. B* **66**, 165205 (2002).
40. E.V. Lavrov, F. Börrnert, and J. Weber, *Phys. Rev. B* **71**, 035205 (2005).
41. L.E. Halliburton, L. Wang, L. Bai, N.Y. Garces, N.C. Giles, M.J. Callahan, B. Wang, *J. Appl. Phys.* **96**, 7168 (2004).
48. G. Alvin Shi, M. Saboktakin, M. Stavola, and S.J. Pearton, *Appl. Phys. Lett.* **85**, 5601-3 (2004).
49. D. Loss and D.P. DiVincenzo, "Quantum computation with quantum dots," *Phys. Rev. A* **57**, 120-6 (1998).
50. J.A. Gupta, D.D. Awschalom, X. Peng, and A.P. Alivisatos, "Spin coherence in semiconductor quantum dots," *Phys. Rev. B* **59**, R10421-4 (1999).
51. P. Mulvaney, "Optical properties of some nanocrystal doped glasses and polymers," *Glass Science and Technology* **75**, 310-8, Suppl. C1 (2002).
52. J.M. Elzerman, R. Hanson, L.H. Willems van Beveren, B. Witkamp, L.M.K. Vandersypen, and L.P. Kouwenhoven, "Single-shot read-out of an individual electron spin in a quantum dot," *Nature* **430**, 431-5 (2004).
53. W.M. Hlaing Oo, M.D. McCluskey, A.D. Lalonde, and M.G. Norton, *Appl. Phys. Lett.* **86**, 073111 (2005).
54. C.G. Van de Walle, private communication.